Applied Nanoscience
https://doi.org/10.1007/s13204-021-01780-0

ORIGINAL ARTICLE

Electrodeposited nickel–graphene nanocomposite coating: influence of graphene nanoplatelet size on wear and corrosion resistance

Tran Van Hau[1,2] · Pham Van Trinh[1] · Nguyen Van Tu[1] · Phan Nguyen Duc Duoc[4] · Mai Thi Phuong[1] · Nguyen Xuan Toan[3,5] · Doan Dinh Phuong[1,3] · Nguyen Phuong Hoai Nam[2] · Vu Dinh Lam[3] · Phan Ngoc Minh[3] · Bui Hung Thang[1,3]

Received: 17 November 2020 / Accepted: 4 March 2021

Abstract
In this paper, we broaden our previous work, which investigated the influence of graphene nanoplatelets (GNPs) size on microstructure and hardness of composite coatings, to determine the effect of GNP size on wear-resistance and anti-corrosion property of GNP-reinforced nickel coating (Ni/GNPs). The experimental results indicated that the small GNP material size could enhance the wear resistance for nickel composite coating with the wear rate of 13.2×10^{-4} mm^3/Nm, the wear depth of 17.69 µm. Meanwhile, the anti-corrosion property is enhanced significantly, this is shown via the low corrosion current density (I_{corr} value of 1.16×10^{-7} A/cm^2) and the high corrosion potential (E_{corr} value of − 0.1661 V). In addition, the mass lost in salt fog testing is low with the weight of 12.3 mg, which decreased down to ~ 55.27% compared to pristine Ni coating. These results are attributed to the uniform distribution of the small GNP size inside Ni matrix as well as the grain refinement effect of composite coating when using the small GNP size.

Keywords Graphene nanoplatelets · Electrodeposition Ni coating · Wear resistance · Anti-corrosion

Introduction

Nickel is a common metal used to protect the surface of conductive materials from wear and corrosion by electroplating method, because it owns many good mechanical and electrochemical properties (Suresh et al. 1993; Reid 2001; Lupi and Pilone 2001; Torrents et al. 2010; Höppel and Göken 2011; Rashmi et al. 2017). In the past few decades, there are various attempts widening previous studies and measures could be implemented to enhance the anti-corrosion and wear resistance for the nickel coating. One of these methods is that particles which have a higher microhardness are used to reinforce the nickel coating such as SiC, Al_2O_3, TiO_2, SiO_2 or carbon nanomaterials (graphene and carbon nanotubes) (Musil 2000; Holubar et al. 2000; Andrievski 2001). Among these reinforced materials, graphene is attracting more attention from researchers than other materials owing to its unique mechanical properties including an intrinsic mechanical strain of ~ 25% and Young's modulus of 1.0 TPa, tensile strength of 130 GPa, large surface area (Novoselov et al. 2005; Lee et al. 2008; Dai et al. 2015; Papageorgiou et al. 2017).

There were a high number of papers about the graphene-reinforced nickel coating related to anti-corrosion and wear resistance, which were published from 2013 to presence. All those results showed the higher anti-corrosion and wear-resistance property of the graphene-reinforced nickel composite compared to the pure nickel coating. In 2015, Algul et al. studied the influence of graphene content on

✉ Tran Van Hau
hautv@ims.vast.ac.vn

✉ Bui Hung Thang
thangbh@ims.vast.vn

1 Institute of Materials Science, Vietnam Academy of Science and Technology, 18 Hoang Quoc Viet Str., Cau Giay Distr., Hanoi, Vietnam

2 VNU University of Engineering and Technology, 144 Xuan Thuy Str., Cau Giay Distr., Hanoi, Vietnam

3 Graduate University of Science and Technology, Vietnam Academy of Science and Technology, 18 Hoang Quoc Viet Str., Cau Giay Distr., Hanoi, Vietnam

4 Department of Physics, Nha Trang University, 02 Nguyen Dinh Chieu Str., Nha Trang, Vietnam

5 Centre for Technology Environmental Treatment, 282 Lac Long Quan Str., Tay Ho Distr., Hanoi, Vietnam

Published online: 20 March 2021

the wear-resistance property of nickel/graphene coating via pulse electrodeposition method (Algul et al. 2015). Chen et al. reported the tribological behavior of nickel/graphene under room temperature in 2016 (Chen et al. 2016). In that time, Szeptycka et al. published the research on graphene-based nickel coating with corrosion resistance properties (Szeptycka et al. 2016). In recent years, there are many of studies focusing on the change of electrodeposition technique so as to enhance the anti-corrosion and wear resistance for nickel/graphene coating (Li et al. 2014, 2016; Jabbar et al. 2017; Yasin et al. 2018a, b, c, 2020; Liu et al. 2018; Singh et al. 2018).

In our previous study, the influence of graphene nanoplatelet size on the microstructure and hardness of nickel/graphene coating was investigated elaborately (Van Hau et al. 2020). Thus, this work, we have broadened our previous study, which the influence of graphene nanoplatelet sizes on the wear-resistance and anti-corrosion properties is studied in detail.

Experimental

Preparation of Ni/GNP nanocomposite coatings

Commercial GNPs (ACS, diameter: 5–7 μm, thickness: 10–15 nm) were modified by ball-milling technique with different times to obtain various GNP sizes (GNPs1; GNPs3; GNPs5 correspond to the milling time of 1 h, 3 h and 5 h), which are described elaborately in the previous study (Van Hau et al. 2020). Milled GNPs with various sizes had been functionalized with carboxyl groups (–COOH) via the strong oxidizing agent including acid HNO_3 and H_2SO_4 with the volume ratio of 1:3 [process was described at works Thang et al. 2014; Van Trinh et al. 2018; Van Hau et al. 2019)] before they were dispersed homogeneously in 1-l Watts solution including 300 g $NiSO_4 \cdot 6H_2O$, 50 g $NiCl_2 \cdot 6H_2O$, 40 g H_3BO_3 and 0.1 g sodium dodecyl sulfate (SDS). The graphene-reinforced nickel nanocomposite coating (Ni/GNPs1; Ni/GNPs3; Ni/GNPs5) was fabricated by electrodeposition method with the conditions described in Table 1. Nickel coating was also prepared by the same process without the GNP content.

Wear-resistance and anti-corrosion test

Wear-resistance test was performed at room temperature by BEVS 2803 equipment which uses the ball-on-flat configurations (Fig. 1). Counter materials used in this test were chromium bearing steel ball with diameter of 8 mm and microhardness of 700–900 HV. Testing parameters are shown in Table 2.

To estimate the wear rate, we used following equations:

Table 1 Parameter of electrodeposition process

Plating parameter	
Current density	2.5 A/dm^2
Temperature	45 °C
pH	4–5
Stirring speed	100 rpm
Plating time	90 min
Watts solution	1 l
GNP sample	GNPs1; GNPs3; GNPs5
GNP concentration	0.3 g/l

$$S = \frac{1}{2}WR - \frac{W\sqrt{4R^2 - W^2}}{4} \quad (1)$$

where S is the cross-section area and W is the width of wear track; R is the ball radius;

$$V = S.L \quad (2)$$

where V is the volume; L is the length of track;

$$Q = \frac{V}{F_N.D} \quad (3)$$

in which Q is the wear rate; F_N is the normal force; and D is the sliding distance.

Potentiodynamic polarization curves were tested in 3.5% sodium chloride solution so as to determine the anti-corrosion property of Ni/GNP nanocomposite coating. This test was carried using a Autolab PGSTAT302N equipment with the surface area of tested samples were 1 cm^2, the scanning rate was 1 mV/s. Salt fog test followed the JIS H8502:1999 standard (Japan) was carried in 5% sodium chloride solution with conditions as follows: pH range 6.5–7.2; spraying pressure of 1.0 atm; temperature: 35–37 °C, testing time of 96 h.

Characterization techniques

Surface-coating roughness was examined using SRT-6200 digital surface roughness tester. Wear tracks of Ni/GNP nanocomposite coating were evaluated the morphology and component via Field-emission scanning electron microscopy (FE-SEM, S-4800; Hitachi, Japan) equipped with an energy-dispersive spectroscopy (EDS). An Axiovert 40MAT equipment from Carl Zeiss, Germany was employed to consider the cross-section of wear tracks. A LabRAM HR 800 (HORIBA Jobin Yvon, France) was used to investigated Raman spectral. Salt fog testing was performed via Q-FOG CCT 600 equipment (USA).

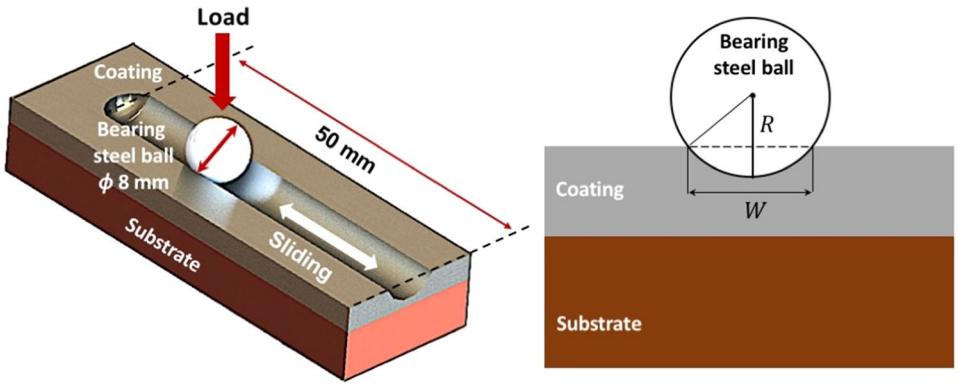

Fig. 1 The wear test process

Table 2 Testing parameters

Sample tested	Testing conditions			
	Counter material	Load	Speed	Sliding distance
Ni				
Ni/GNPs1	Chromium bearing steel ball ϕ 8 mm	1; 2; 3; 4; 5 N	5 cm/s	50 m
Ni/GNPs3				
Ni/GNPs5				

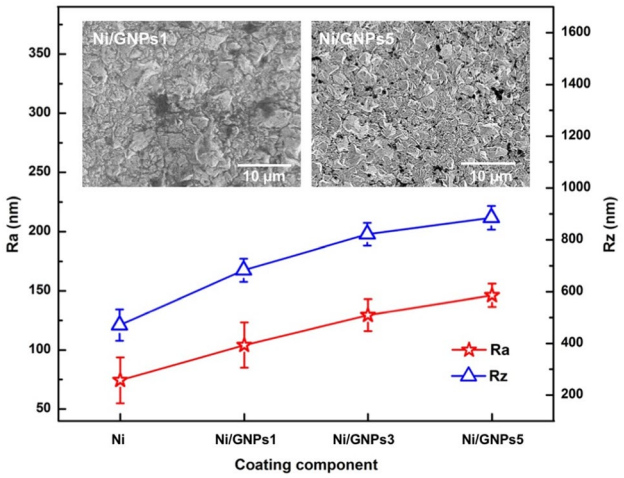

Fig. 2 Surface morphology and roughness of Ni/GNP nanocomposite coatings and pristine Ni coating

Results and discussion

Surface morphology and roughness

Figure 2 shows the surface morphology and roughness of nanocomposite coatings. The surface roughness rises with decreasing the GNP size, the arithmetical mean roughness (Ra) increases from around 75 nm to about 145 nm corresponding to Ni and Ni/GNPs5 coating, meanwhile the ten-point mean roughness (Rz) climbs from 470 to 880 nm. The reason for these results is expected due to the formation of a grain refinement effect of composite coating. FE-SEM images inserted in Fig. 2 indicated the significant difference of surface morphology between Ni/GNPs1 and Ni/GNPs5, this is attributed to the influence of small size of GNP materials leading to a fine grain size of Ni/GNPs5 nanocomposite coating, which was explained elaborately in previous work (Van Hau et al. 2020). This is one of the primary reasons for the increase of microhardness of Ni/GNPs5 coating compared to Ni and Ni/GNPs1 coatings from 186 HV (for Ni coating) and 229 HV (for Ni/GNPs1) to 273 HV (for Ni/GNPs5).

Morphology of wear track

Figure 3 is the FE-SEM image of the worn surface of composite coatings with the low magnification measured at load condition of 5 N. This result shows the influence of GNP sizes on the wear-resistance property of composite coating. As can be seen clearly that the width of wear tracks decrease slightly when GNP sizes decline (Table 3), this results in a reduction of the worn volume. Figure 3a shows that, the pristine Ni coating surface was damaged severely when it was worn. The surface of wear track revealed a lot of signs of serious cutting, deep ploughing and push-ups on the bottom of the wear track. This indicated that the mechanism of adhesive wear impacted significantly during testing process. Figure 3b–d is the surface morphology of the wear track of

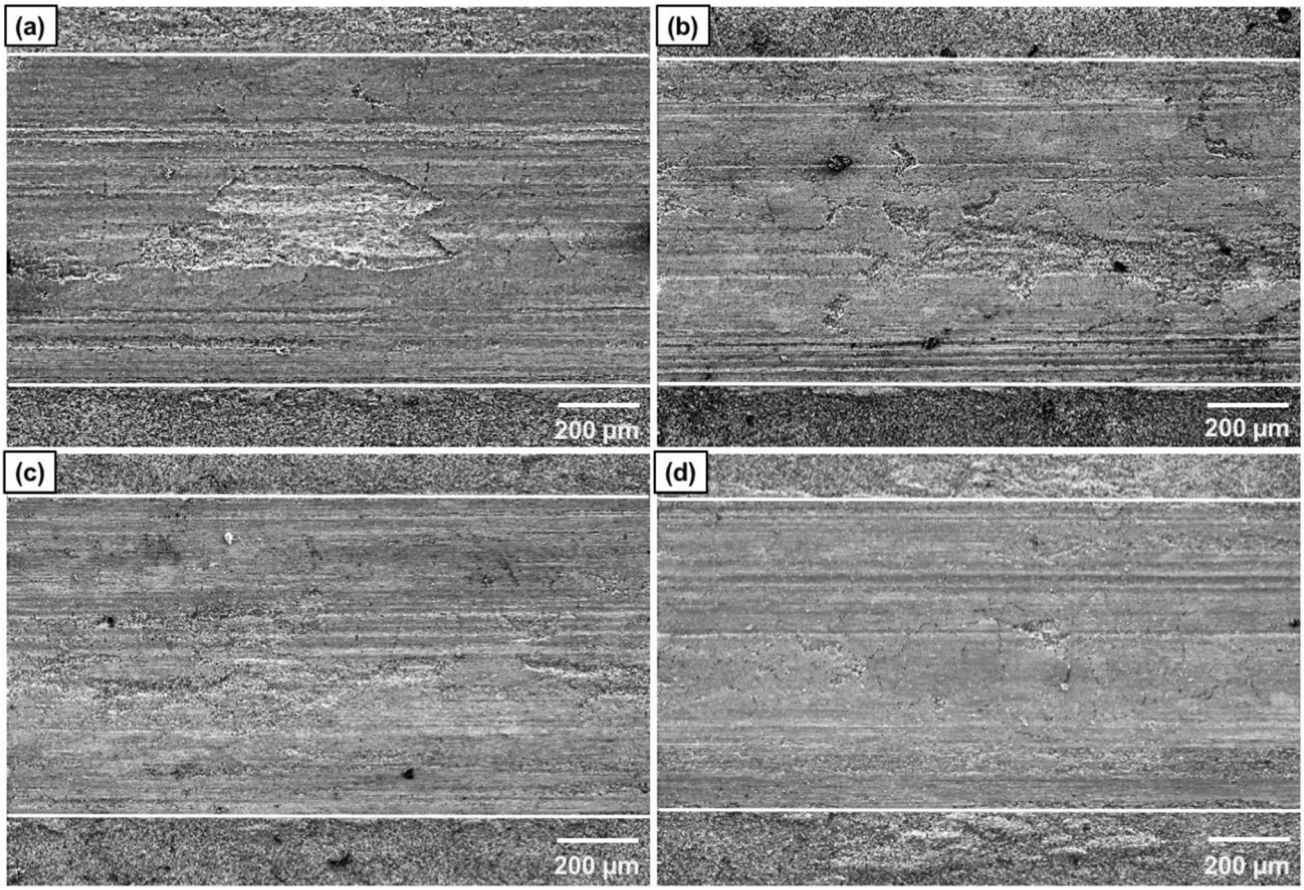

Fig. 3 Low magnification FE-SEM images of wear track of composite coatings (**a**) Ni, (**b**) Ni/GNPs1, (**c**) Ni/GNPs3, and (**d**) Ni/GNPs5 measured at load condition of 5 N

Table 3 Width of wear track of coatings measured at load conditions of 5 N

Sample tested	Width of track (µm)
Ni	795
Ni/GNPs1	770
Ni/GNPs3	761
Ni/GNPs5	751

Ni/GNPs1, Ni/GNPs3, and Ni/GNPs5, respectively. Similarly to the worn surface of Ni coating, the wear track of Ni/GNPs1 showed a considerable destruction with a large scar and deep furrows in surface. However, when using the smaller GNP sizes to reinforce nickel coatings (Ni/GNPs3 and Ni/GNPs5), the wear track showed that the worn surface was smoother and the furrows were smaller and shallower.

Figure 4 is the FE-SEM image with high magnification of the worn surface of nanocomposite coatings measured at load condition of 5 N. It is obvious that the worn surfaces changed dramatically when using the different reinforced material sizes. Figure 4a shows that the surface of Ni coating was damaged heavily with large scars, wide cracks and push-ups on the bottom. There was an enormously delamination due to the mechanism of adhesive wear. The wear-resistance property of nickel coatings were improved significantly when they were reinforced GNP materials, this was demonstrated in Fig. 4b–d. As can be seen, the surface destruction of GNP-reinforced nickel coatings due to the mechanism of adhesive wear decreased considerably. Simultaneously, the width of cracks tends to narrow with decreasing the GNP sizes. In addition, the surface of wear tracks became gradually smoother and appearing a lot of debris, which indicates the mild abrasive wear phenomena.

To evaluate more elaborately about the wear-resistance property of the nickel coating reinforcing the GNP materials with different sizes, the cross-section of wear track of coatings were examined, the result is shown in Fig. 5 indicating that the depth of wear track of coatings decrease with decreasing the size of GNP material. Namely, for Ni coating, the track depth was 19.79 µm (Fig. 5a). In the case of Ni/GNP coatings (Fig. 5b–d), the depth was 18.57 µm, 18.17 µm, and 17.69 µm corresponding to Ni/GNPs1, Ni/

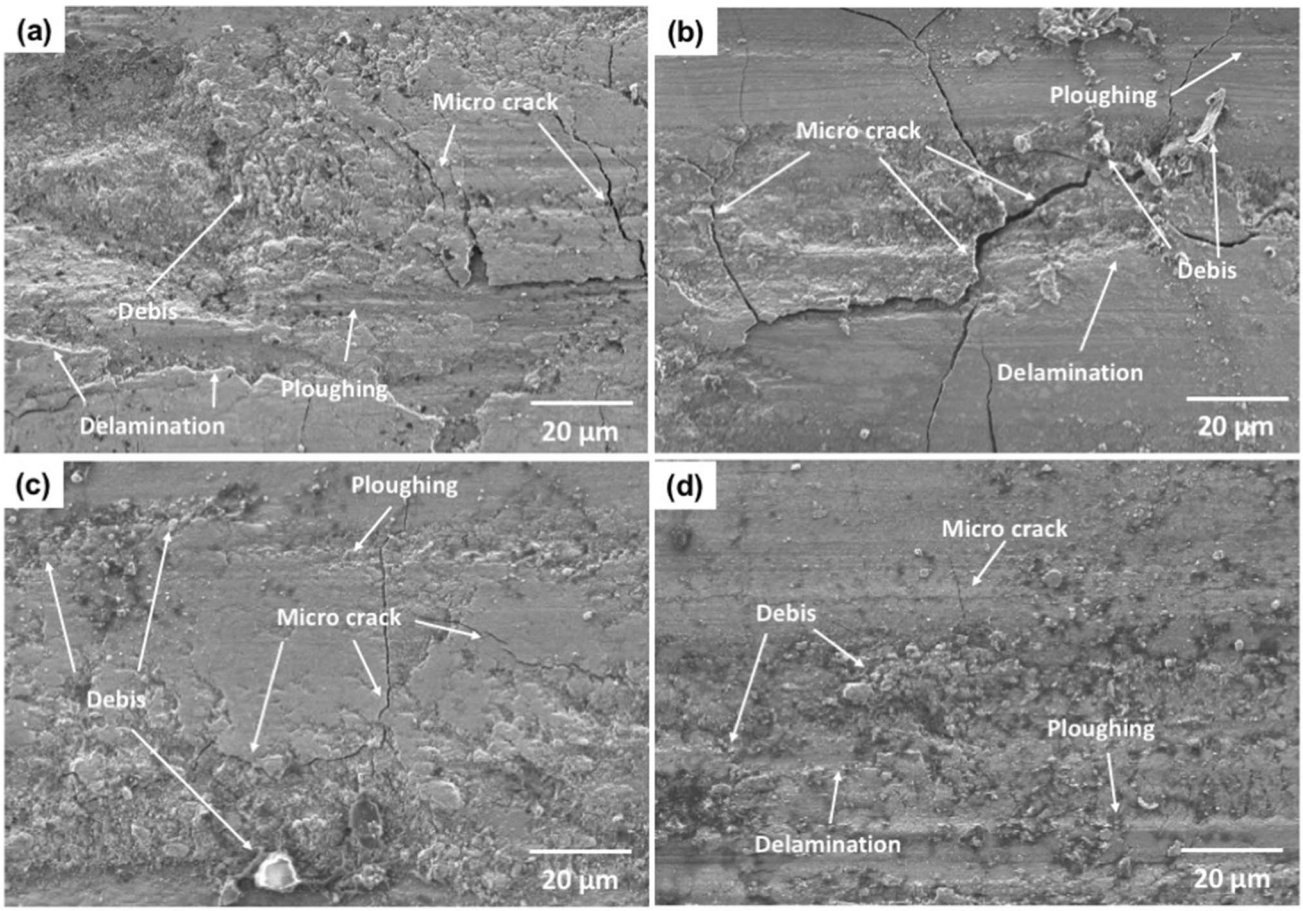

Fig. 4 High magnification FE-SEM images of wear track of composite coatings (**a**) Ni, (**b**) Ni/GNPs1, (**c**) Ni/GNPs3, and (**d**) Ni/GNPs5 measured at load condition of 5 N

GNPs3, and Ni/GNPs5 coatings. This result demonstrated that Ni/GNPs5 coating had a high wear-resistance property.

Content analysis results at wear track of Ni/GNP coating

Content analysis results at the worn surface of coatings are shown in Fig. 6. Analysis indicated that all of wear tracks contain oxygen element with high percentage. This suggested that the surface of coatings were oxidized significantly. In addition, there was a little Fe component in all the wear track of the coatings, this was attributed to debris of the counter material. Figure 6b–d revealed the presence of carbon nanomaterial in the worn surface. However, carbon component increased from 10.70 to 18.07% corresponding to Ni/GNPs1 and Ni/GNPs5, the reason for this is the Ni/GNPs5 coating is high in GNP component, which was demonstrated in our previous study (Van Hau et al. 2020). Figure 7 is the Raman spectral of GNP material measured at the various positions in the wear track. Results showed the significant impact of wear process on GNP material of Ni/GNPs5 coating. As can be seen, the characterized peaks of GNP materials appeared including G peak (at wavenumber of 1580 cm^{-1}) and D peak (around band of 1340 cm^{-1}). However, there was a change of D peak at the central site of wear track (position 2). Investigating I_D/I_G ratio to evaluate the damage level of GNP materials (Reina et al. 2009; Dong et al. 2011; Nguyen et al. 2013), result demonstrated that GNP materials at the position 2 was damaged dramatically with the high defect level (I_D/I_G ratio of 1.07). Meanwhile, at the boundary of wear track, the damage level of GNP materials was lower with I_D/I_G ratio of 0.801 and 0.806 corresponding to position 1 and position 3. This proved that the wear process took place dramatically at center site of coatings. In addition, there was a strong redshift of D peak and a weak redshift of G peak in Raman spectral at position 2 and position 3, this attributed to the impact of wear test leading to the deformed GNP structure. This was demonstrated in previous works (del Corro et al. 2012; Zheng et al. 2015). However, the shift of D peak is stronger than that of G peak, which has not been focus on our current study. This

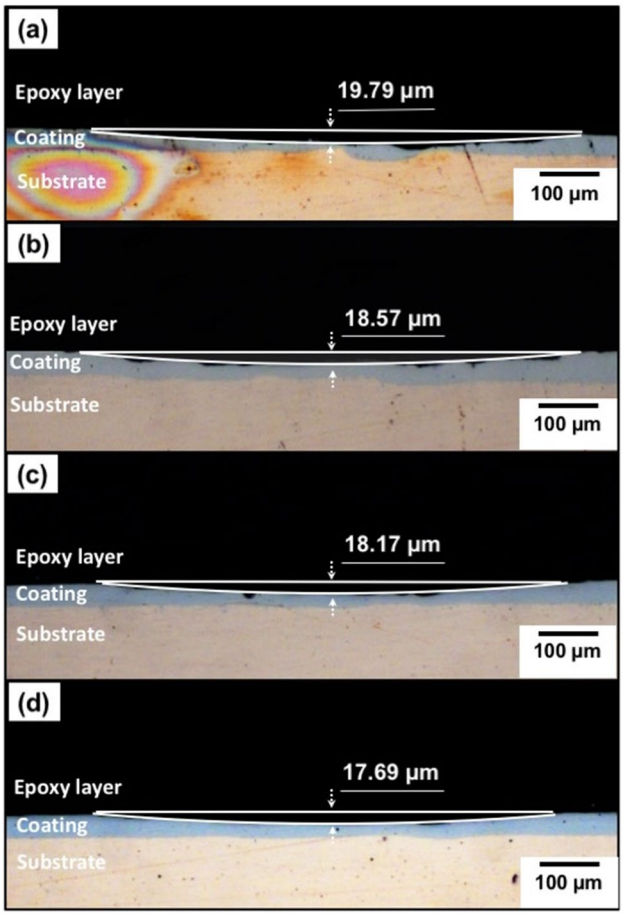

Fig. 5 Cross-sectional optical images of wear tracks of coatings (**a**) Ni, (**b**) Ni/GNPs1, (**c**) Ni/GNPs3, and (**d**) Ni/GNPs5 measured at load condition of 5 N

will be studied more elaborately in later works to evaluate the change of GNP structure due to the impact of wear test.

Influence of GNP sizes on wear rate of Ni/GNP coating

Based on Eqs. (1)–(3), we estimated the wear rate of coatings including Ni, Ni/GNPs1, Ni/GNPs3, Ni/GNPs5 with various load condition ranging from 1 to 5 N. Results are shown in Fig. 8 indicating that the wear rate increased considerably with increasing the load conditions (from 1 to 5 N). It is obvious that the wear rate of Ni/GNPs5 coating was lowest with respect to all of load conditions, this result showed clearest at load condition 5 N, namely for Ni/GNPs5 coatings, the wear rate was about 13.2×10^{-4} mm^3/Nm whereas the Ni/GNPs3, Ni/GNPs1 and Ni coatings were around 13.8×10^{-4} mm^3/Nm, 14.3×10^{-4} mm^3/Nm and 15.7×10^{-4} mm^3/Nm, respectively. This result carries two meanings, the first one is the GNPs5 material helps nickel coating enhance more the wear resistance than other GNP material sizes. Second, the influence of GNP sizes on the wear rate was observed most obviously at the load condition of 5 N.

There are a number of reasons for the wear rate reduction of Ni/GNPs5 coatings. The first reason is the nickel matrix was reinforced GNPs5 material leading to increase the microhardness for composite coating, which demonstrated in our previous study. The increase of microhardness contributes to enhancing the wear-resistance property for composite coating which was described via Archard's principle (Qi et al. 2019; Xiang et al. 2019). Another reason is the high concentration and uniform dispersion of graphene content inside nickel matrix (Van Hau et al. 2020) result in the reduction in friction and the improvement of the wear-resistance property of composite. It is known that carbon nanomaterial including graphene, carbon nanotubes, fullerene plays important role in the reduction of friction coefficient, which reported elaborately in these works (Shao et al. 2012; Chen et al. 2016; Singh et al. 2018).

Influence of GNP sizes on anti-corrosion property of Ni/GNP coating

Potentiodynamic polarization curves of coatings including Ni, Ni/GNPs1, Ni/GNPs3, and Ni/GNPs5 coatings (Fig. 9) were investigated to evaluate the anti-corrosion property. Parameters including corrosion potentials (E_{corr}) and current densities (I_{corr}) derived from Fig. 9 are shown in Table 4. As can be seen, all the graphene-reinforced nickel coatings had the higher E_{corr} and the lower I_{corr} compared to the Ni coating. This was attributed to the presence of graphene component inside nickel matrix, which was demonstrated elaborately in previous works (Kumar et al. 2013; Szeptycka et al. 2016; Yasin et al. 2018b). In addition, the influence of GNP material sizes on anti-corrosion of composite coatings was also revealed in Table 4. It is clearly that the anti-corrosion property of Ni/GNPs5 coating is highest with the I_{corr} value of 1.16×10^{-7} A/cm^2 and E_{corr} value of − 0.1661 V whereas the values of I_{corr} and E_{corr} of the Ni/GNPs1 and Ni/GNPs3 coatings is 5.50×10^{-7} A/cm^2 and − 0.2582 V; 3.93×10^{-7} A/cm^2 and − 0.2109 V, respectively, which indicated the lower anti-corrosion property of the Ni/GNPs1 and Ni/GNPs3 coatings. Figure 10 is the optical images of coatings including Ni, Ni/GNPs1, Ni/GNPs3, and Ni/GNPs5 before and after the salt fog testing for 96 h. Result exhibited the sign of corrosion in the surface of all composite coating. By the optical images, it is easy to recognize that Ni coating was corroded highest, meanwhile Ni/GNPs5 coating was corroded lowest. To evaluate more elaborately, we considered the mass lost of coatings, results are shown in Fig. 11. It is obviously that Ni coating was corroded heavily with the mass lost about 27.5 mg whereas the graphene-reinforced nickel coatings had a lower mass lost, namely the mass lost

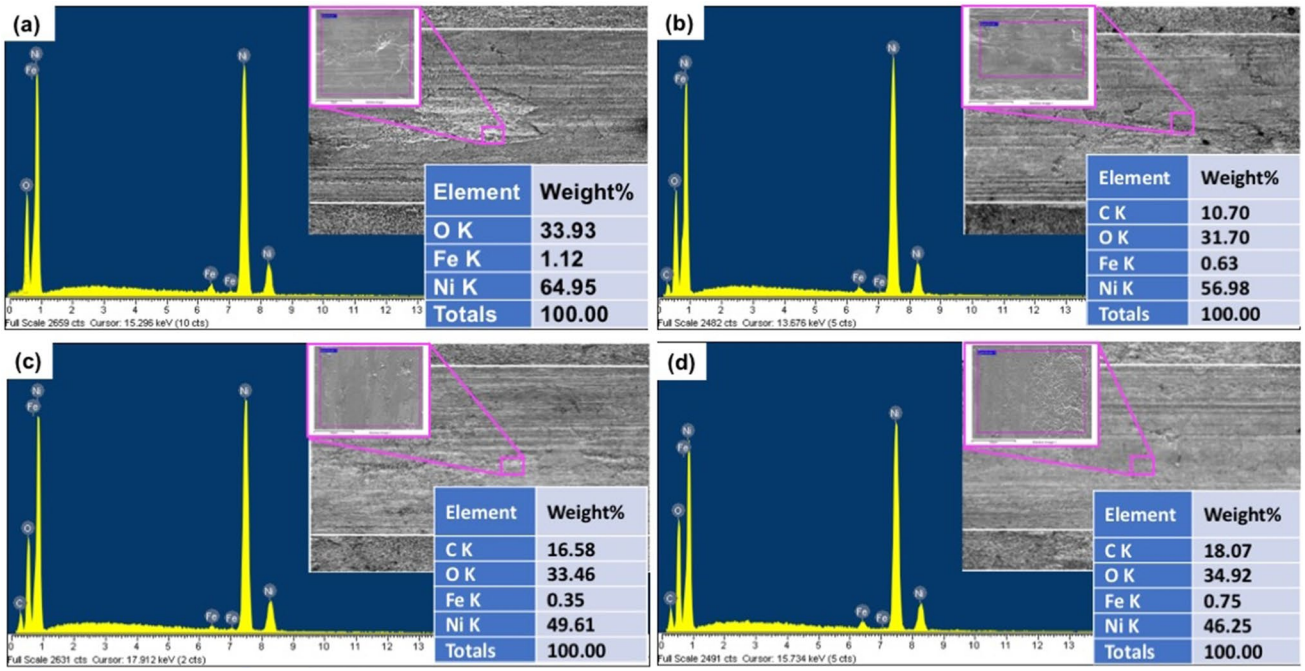

Fig. 6 EDS analysis results in the wear track of coatings (**a**) Ni, (**b**) Ni/GNPs1, (**c**) Ni/GNPs3, and (**d**) Ni/GNPs5 measured at load condition of 5 N

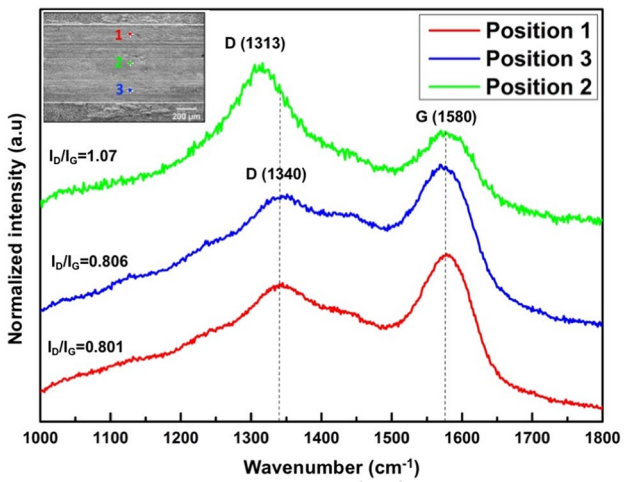

Fig. 7 Raman spectra of Ni/GNPs5 coating at various position in the wear track measured at load condition of 5 N

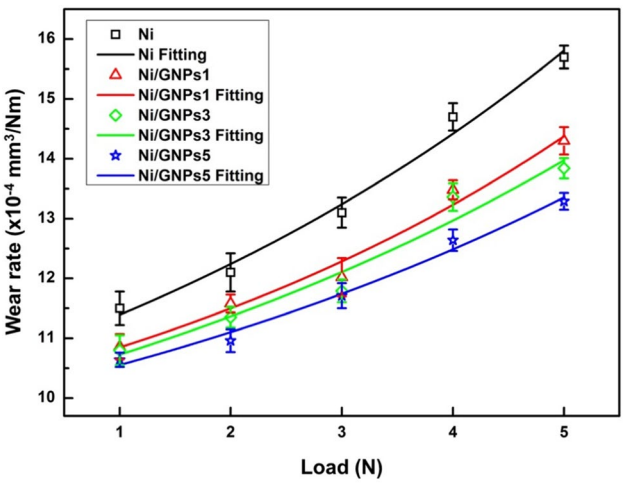

Fig. 8 Wear rate of the nickel coating and the graphene-reinforced nickel coatings

of the Ni/GNPs1, Ni/GNPs3, and Ni/GNPs5 coatings were 19.3 mg, 16.6 mg and 12.3 mg, respectively. Compared to the Ni coating, the mass lost of Ni/GNPs5 reduced 55.27% meanwhile the Ni/GNPs1 coating decreased 29.81% and the Ni/GNPs3 coatings declined 39.64%.

Generally, there are various factors that influence on the anti-corrosion property of coatings including the chemical component of plating solutions (Yasin et al. 2018b), plating technique (current density, temperature of plating process Jabbar et al. 2017; Yasin et al. 2018b)), crystallite size of metal matrix (Alizadeh and Cheshmpish 2019), the presence of graphene content (Kumar et al. 2013) as well as it concentration (Yasin et al. 2018c). The influence of GNP material sizes on the anti-corrosion property could be explained as follows: The dispersed ability of GNP materials in Watts solution tend to increase when their sizes are small, this leads to the high content and uniform distribution of GNP material inside nickel matrix, which demonstrated

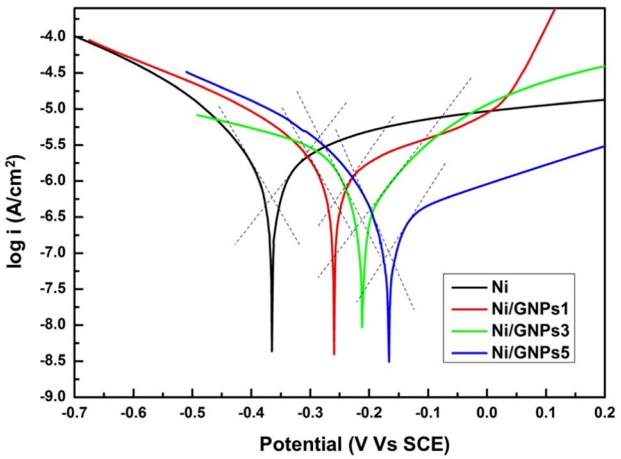

Fig. 9 Potentiodynamic polarization curve of coatings including Ni, Ni/GNPs1, Ni/GNPs3, and Ni/GNPs5 coatings

Table 4 Corrosion potentials (E_{corr}) and current densities (I_{corr}) were derived from potentiodynamic polarization curves of coatings

Sample tested	E_{corr} (V)	I_{corr} (A/cm^2)
Ni	– 0.3653	6.17×10^{-7}
Ni/GNPs1	– 0.2582	5.50×10^{-7}
Ni/GNPs3	– 0.2109	3.393×10^{-7}
Ni/GNPs5	– 0.1661	1.16×10^{-7}

elaborately in our previous work (Van Hau et al. 2020). In addition, in our previous work, we had already demonstrated that the crystallite sizes of nickel reaches a grain refinement when the GNP material size is small. This is one of the reason leading to the high anti-corrosion property of Ni/GNPs5 coating. According to a report of Cui et al. (2017), graphene is cathodic to most metals including nickel so it can promote corrosion when nickel component cannot completely cover the surface. From this perspective, the small GNP sizes play important role with respect to the anti-corrosion property of GNP-reinforced nickel coatings. In our previous work (Van Hau et al. 2020), by FE-SEM images of GNP–nickel interface, we demonstrated that it is easy for nickel crystallite to cover the whole GNPs5 surface due to its small size. By contrast, for the larger sizes of GNP material (GNPs1, GNPs3), it is difficult for nickel crystallite to cover completely the GNP surface.

Conclusions

Based on our previous work, we have already broadened the investigation of the influence of GNP material size on the wear-resistance and anti-corrosion properties of GNP-reinforced nickel coatings. Results indicated that the small GNP material size could enhance the wear resistance and anti-corrosion for the nickel composite coating. Namely, the Ni/GNPs5 coating has the highest wear resistance and anti-corrosion with the wear depth of 17.69 µm, wear rate of 13.2×10^{-4} mm^3/Nm which decreased down to 15.9% compared to pristine nickel coating. Meanwhile, the obtained corrosion potential and corrosion density current are − 0.1661 V and 1.16×10^{-7} A/cm^2, respectively, in addition, the mass lost in salt fog testing decreased down to ~ 55.27% compared to pristine Ni coating indicating the high anti-corrosion of Ni/GNPs5 coating.

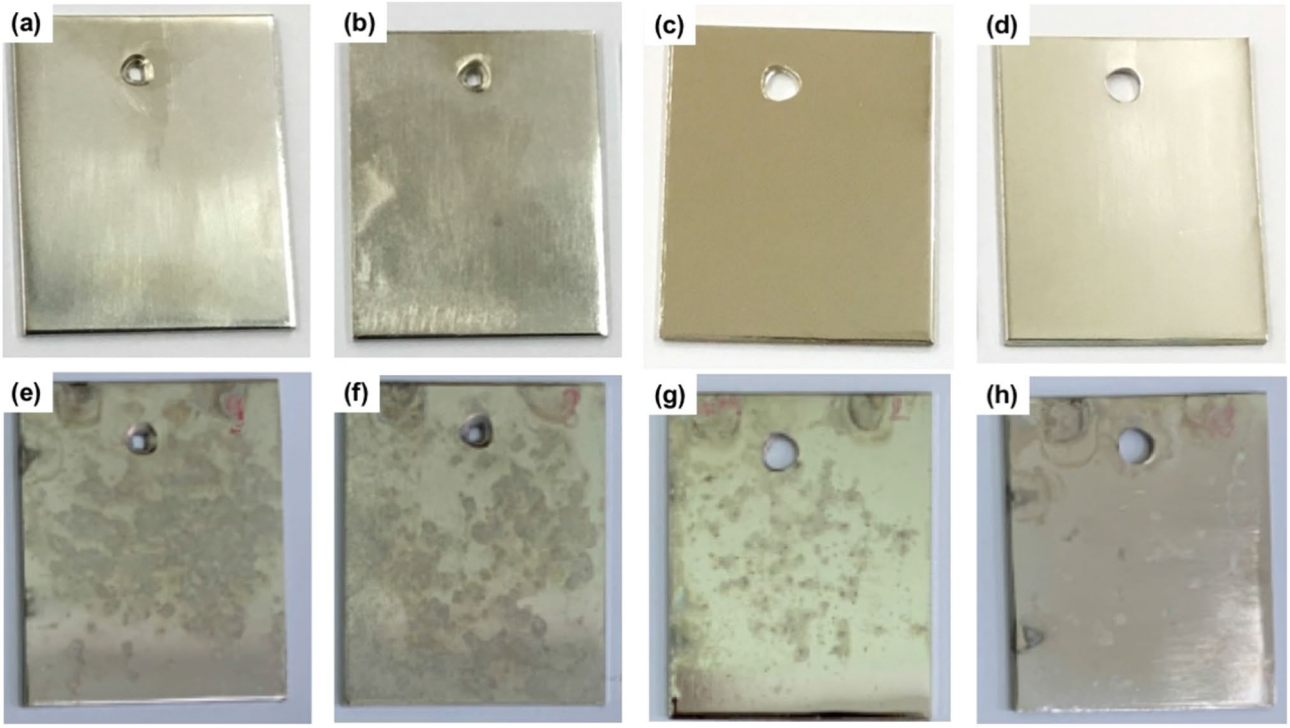

Fig. 10 Optical images of coatings before salt fog testing (**a**) Ni, (**b**) Ni/GNPs1, (**c**) Ni/GNPs3, (**d**) Ni/GNPs5 and after salt fog testing (**e**) Ni, (**f**) Ni/GNPs1, (**g**) Ni/GNPs3, (**h**) Ni/GNPs5 with testing time of 96 h

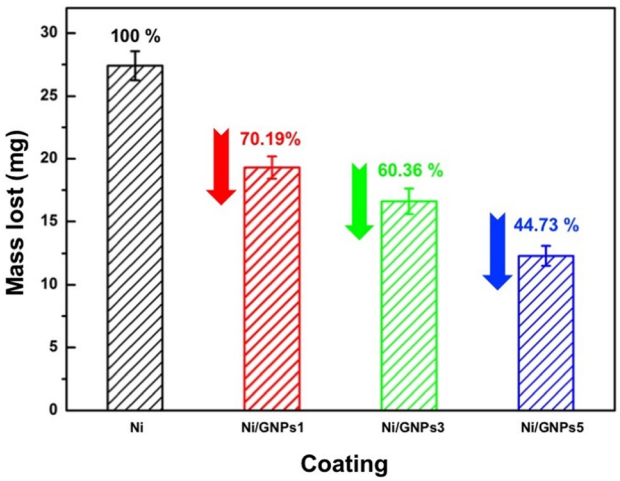

Fig. 11 The mass lost of coatings in salt fog testing with the testing time of 96 h

Funding This research received no external funding.

Declarations

Conflict of interest The authors declare no conflict of interest.

References

Algul H, Tokur M, Ozcan S et al (2015) The effect of graphene content and sliding speed on the wear mechanism of nickel–graphene nanocomposites. Appl Surf Sci 359:340–348. https://doi.org/10.1016/j.apsusc.2015.10.139

Alizadeh M, Cheshmpish A (2019) Electrodeposition of Ni-Mo/Al_2O_3 nano-composite coatings at various deposition current densities. Appl Surf Sci 466:433–440. https://doi.org/10.1016/j.apsusc.2018.10.073

Andrievski R (2001) Films as nanostructured materials with characteristic mechanical properties. Mater Trans 42:1471–1473. https://doi.org/10.2320/matertrans.42.1471

Chen J, Li J, Xiong D et al (2016) Preparation and tribological behavior of Ni–graphene composite coating under room temperature. Appl Surf Sci 361:49–56. https://doi.org/10.1016/j.apsusc.2015.11.094

Cui C, Lim ATO, Huang J (2017) A cautionary note on graphene anti-corrosion coatings. Nat Nanotechnol 12:834–835. https://doi.org/10.1038/nnano.2017.187

Dai JF, Wang GJ, Ma L, Wu CK (2015) Surface properties of graphene: relationship to graphene-polymer composites. Rev Adv Mater Sci 40:60–71

del Corro E, Taravillo M, Baonza VG (2012) Nonlinear strain effects in double-resonance Raman bands of graphite, graphene, and related materials. Phys Rev B 85:033407. https://doi.org/10.1103/PhysRevB.85.033407

Dong X, Wang P, Fang W et al (2011) Growth of large-sized graphene thin-films by liquid precursor-based chemical vapor deposition under atmospheric pressure. Carbon N Y 49:3672–3678. https://doi.org/10.1016/j.carbon.2011.04.069

Holubar P, Jilek M, Sima M (2000) Present and possible future applications of superhard nanocomposite coatings. Surf CoatTechnol

133–134:145–151. https://doi.org/10.1016/S0257-8972(00)00956-7
Höppel HW, Göken M (2011) The processing of bulk nanocrystalline metals and alloys by electrodeposition. In: Whang SH (ed) Nanostructured metals and alloys. Woodhead Publishing, Cambridge, pp 507–541
Jabbar A, Yasin G, Khan WQ et al (2017) Electrochemical deposition of nickel graphene composite coatings: effect of deposition temperature on its surface morphology and corrosion resistance. RSC Adv 7:31100–31109. https://doi.org/10.1039/C6RA28755G
Kumar CMP, Venkatesha TV, Shabadi R (2013) Preparation and corrosion behavior of Ni and Ni–graphene composite coatings. Mater Res Bull 48:1477–1483. https://doi.org/10.1016/j.materresbull.2012.12.064
Lee C, Wei X, Kysar JW, Hone J (2008) Measurement of the elastic properties and intrinsic strength of monolayer graphene. Science 321:385–388. https://doi.org/10.1126/science.1157996
Li M, Che H, Liu X et al (2014) Highly enhanced mechanical properties in Cu matrix composites reinforced with graphene decorated metallic nanoparticles. J Mater Sci 49:3725–3731. https://doi.org/10.1007/s10853-014-8082-x
Li J, An Z, Wang Z et al (2016) Pulse-reverse electrodeposition and micromachining of graphene–nickel composite: an efficient strategy toward high-performance microsystem application. ACS Appl Mater Interfaces 8:3969–3976. https://doi.org/10.1021/acsami.5b11164
Liu Y, Liu Y, Zhang Q et al (2018) Control of the microstructure and mechanical properties of electrodeposited graphene/Ni composite. Mater Sci Eng A 727:133–139. https://doi.org/10.1016/j.msea.2018.04.092
Lupi C, Pilone D (2001) Electrodeposition of nickel–cobalt alloys: the effect of process parameters on energy consumption. Miner Eng 14:1403–1410. https://doi.org/10.1016/S0892-6875(01)00154-6
Musil J (2000) Hard and superhard nanocomposite coatings. Surf Coat Technol 125:322–330. https://doi.org/10.1016/S0257-8972(99)00586-1
Nguyen VT, Le HD, Nguyen VC et al (2013) Synthesis of multi-layer graphene films on copper tape by atmospheric pressure chemical vapor deposition method. Adv Nat Sci Nanosci Nanotechnol. https://doi.org/10.1088/2043-6262/4/3/035012
Novoselov KS, Geim AK, Morozov SV et al (2005) Two-dimensional gas of massless Dirac fermions in graphene. Nature 438:197–200. https://doi.org/10.1038/nature04233
Papageorgiou DG, Kinloch IA, Young RJ (2017) Mechanical properties of graphene and graphene-based nanocomposites. Prog Mater Sci 90:75–127. https://doi.org/10.1016/j.pmatsci.2017.07.004
Qi S, Li X, Dong H (2019) Reduced friction and wear of electro-brush plated nickel composite coatings reinforced by graphene oxide. Wear 426–427:228–238. https://doi.org/10.1016/j.wear.2018.12.069
Rashmi S, Elias L, Chitharanjan Hegde A (2017) Multilayered Zn–Ni alloy coatings for better corrosion protection of mild steel. Eng Sci Technol Int J 20:1227–1232. https://doi.org/10.1016/j.jestch.2016.10.005
Reid J (2001) Copper electrodeposition: principles and recent progress. Jpn J Appl Phys 40:2650–2657. https://doi.org/10.1143/JJAP.40.2650
Reina A, Jia X, Ho J et al (2009) Large area, few-layer graphene films on arbitrary substrates by chemical vapor deposition. Nano Lett 9:30–35. https://doi.org/10.1021/nl801827v
Shao W, Nabb D, Renevier N et al (2012) Preparation of electrodeposited Ni-CNTs nanocomposite coatings with highly wear and corrosion resistance properties. Adv Mater Res 548:101–104. https://doi.org/10.4028/www.scientific.net/AMR.548.101
Singh S, Samanta S, Das AK, Sahoo RR (2018) Tribological investigation of Ni–graphene oxide composite coating produced by pulsed electrodeposition. Surfaces Interfaces 12:61–70. https://doi.org/10.1016/j.surfin.2018.05.001
Suresh S, Mortensen A, Needleman A (1993) Fundamentals of metal-matrix composites
Szeptycka B, Gajewska-midzialek A, Babul T (2016) Electrodeposition and corrosion resistance of Ni–graphene composite coatings. J Mater Eng Perform 25:3134–3138. https://doi.org/10.1007/s11665-016-2009-4
Thang BH, Van Trinh P, Quang LD et al (2014) Heat dissipation for the Intel Core i5 processor using multiwalled carbon-nanotube-based ethylene glycol. J Korean Phys Soc 65:312–316. https://doi.org/10.3938/jkps.65.312
Torrents A, Yang H, Mohamed FA (2010) Effect of annealing on hardness and the modulus of elasticity in bulk nanocrystalline nickel. Metall Mater Trans A Phys Metall Mater Sci 41:621–630. https://doi.org/10.1007/s11661-009-0147-0
Van Hau T, Van Trinh P, Hoai Nam NP, Lam VD, Minh PN, Thang BH (2019) Enhanced hardness of nickel coating reinforced functionalized carbon nanomaterials via an electrodeposition technique. Mater Res Exp 6(8):0850c4
Van Hau T, Van Trinh P, Hoai Nam NP et al (2020) Electrodeposited nickel–graphene nanocomposite coating: effect of graphene nanoplatelet size on its microstructure and hardness. RSC Adv 10:22080–22090. https://doi.org/10.1039/D0RA03776A
Van Trinh P, Anh NN, Hong NT et al (2018) Experimental study on the thermal conductivity of ethylene glycol-based nanofluid containing Gr–CNT hybrid material. J Mol Liq 269:344–353. https://doi.org/10.1016/j.molliq.2018.08.071
Xiang L, Shen Q, Zhang Y et al (2019) One-step electrodeposited Ni–graphene composite coating with excellent tribological properties. Surf Coat Technol 373:38–46. https://doi.org/10.1016/j.surfcoat.2019.05.074
Yasin G, Arif M, Nizam MN et al (2018a) Effect of surfactant concentration in electrolyte on the fabrication and properties of nickel–graphene nanocomposite coating synthesized by electrochemical co-deposition. RSC Adv 8:20039–20047. https://doi.org/10.1039/c7ra13651j
Yasin G, Arif M, Shakeel M et al (2018b) Exploring the nickel–graphene nanocomposite coatings for superior corrosion resistance: manipulating the effect of deposition current density on its morphology, mechanical properties, and erosion-corrosion performance. Adv Eng Mater 20:1–12. https://doi.org/10.1002/adem.201701166
Yasin G, Khan MA, Arif M et al (2018c) Synthesis of spheres-like Ni/graphene nanocomposite as an efficient anti-corrosive coating; effect of graphene content on its morphology and mechanical properties. J Alloys Compd 755:79–88. https://doi.org/10.1016/j.jallcom.2018.04.321
Zheng X, Chen W, Wang G et al (2015) The Raman redshift of graphene impacted by gold nanoparticles. AIP Adv 5:057133. https://doi.org/10.1063/1.4921316